JOURNAL OF Materials CHEMISTRY

Gas sensing properties of nanocrystalline metal oxide powders produced by a laser evaporation technique

Geraint Williams and Gary S. V. Coles

Department of Electrical and Electronic Engineering, University of Wales Swansea, Singleton Park, Swansea, UK SA2 8PP

Nanosized powders of Al_2O_3, ZrO_2 and SnO_2 have been produced by laser ablation of ceramic samples followed by condensation in a controlled gaseous atmosphere. X-Ray powder diffraction, transmission and scanning electron microscopy have been used to investigate the morphology and structure of the materials. A study of the gas sensing characteristics of thick films prepared from these materials revealed that zirconia based sensors respond to H_2 at a temperature of 100 °C, while thick films of alumina display marked changes in both resistance and capacitance as a function of relative humidity at room temperature. Nanocrystalline SnO_2 sensors respond markedly to mixtures of H_2, CO and CH_4 in the 100–600 °C temperature range and display sensitivity values which are higher than those obtained using SnO_2 powder samples prepared *via* a conventional wet chemistry route. Optimisation experiments showed that sensor characteristics were influenced both by pre-treatment temperature and film thickness.

Introduction

Nanostructured materials are currently attracting increased attention from researchers keen to exploit their properties for the purpose of producing gas sensing films of high sensitivity. One of the main attractions of these materials is that they offer a substantial increase in surface area compared with conventional microcrystalline powders. However, for gas sensors based on polycrystalline ceramic films, where surface reactions produce electrical changes which comprise the sensing mechanism, the importance of grain size is even more significant. Consider a metal oxide such as tin dioxide (SnO_2), which is widely used for gas sensing applications.[1] At elevated temperatures, oxygen adsorbs on the surface of the SnO_2 grains, accompanied by electron abstraction from the conduction band. This process creates an electron depleted surface region (or space charge layer), which represents a barrier to electrical conduction between the SnO_2 grains. A combustible gas can react with the surface oxygen species, allowing electrons to be re-introduced to the surface region leading to a decrease in the depth of the space charge layer. Hence the barrier to intergrain electrical conduction is reduced and the net observed effect is a drop in the bulk resistance of the polycrystalline sensing element.

For most conventional SnO_2 sensing materials, the grain size is considerably greater than the depth of the space charge region and electrical conduction within the bulk is governed by the grain boundaries. However, nanocrystalline materials offer grain sizes where the depletion layer has similar dimensions to the particle radius, and under these conditions electrical conduction is predominantly grain controlled. Thus when the SnO_2 grains are fully depleted of electrons, very low reducing gas concentrations can have a profound effect on intergrain conduction. It is expected that under these conditions the gas sensitivity should be directly influenced by the particle size, so that increasing sensitivity should accompany a decrease in particle size. The two different conditions described above are illustrated schematically in Fig. 1, where the shaded areas represent regions of high resistivity which form a barrier to the conduction of electrons across the grain boundaries.

The benefits of incorporating nanostructured materials in sensor films with the aim of achieving high reducing gas sensitivity has attracted growing interest, culminating in the appearance of several recent research reports in the literature.

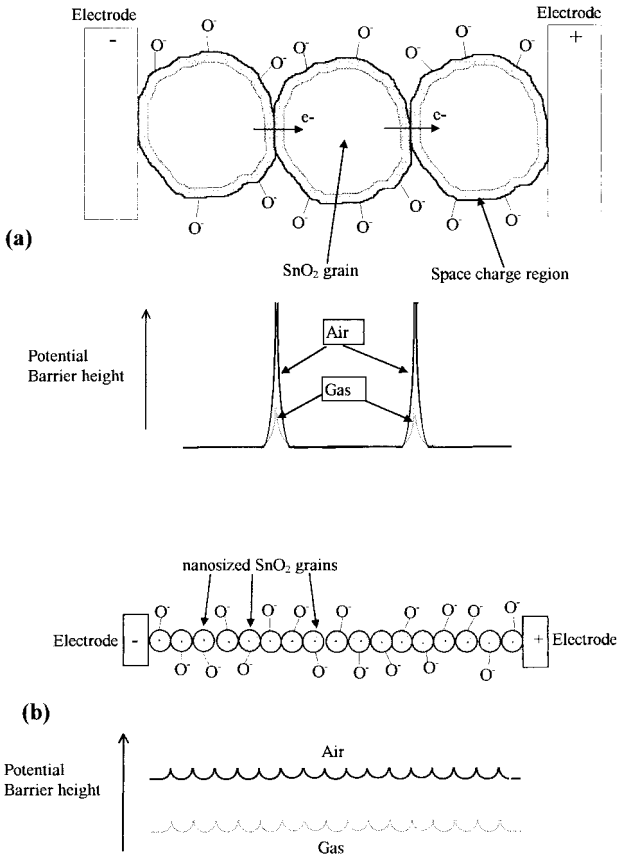

Fig. 1 The influence of SnO_2 particle size on the mechanism of inter grain electron transport for (a) conventional and (b) nanosized materials

Previous studies have relied on a wet chemistry route[2–4] involving the hydrolysis of a metal salt and subsequent grain size regulation by using additives and controlling the calcination temperature of the precipitate. Others have investigated thin films prepared by sputtering methods,[5–8] where close control of parameters such as substrate temperatures during deposition gives rise to a nanostructured active material. In contrast, this paper describes a novel laser evaporation and gas phase condensation method of producing nanocrystalline

oxide powders and outlines some preliminary results obtained for gas sensors prepared from thick films of these materials. Although others have previously used inert gas evaporation methods to prepare nanoscaled SnO and SnO_2 powders,[9] their technique relies on the use of temperatures in excess of 1000 °C to vaporise the precursor material in He gas at reduced pressure. Employing a laser to impart the necessary energy to evaporate the sample allows powder preparation to be conveniently carried out in air at room temperature and atmospheric pressure.

Gas sensor films were prepared from nanocrystalline powders of three different materials produced by this technique, namely alumina (Al_2O_3), zirconia (ZrO_2) and SnO_2. The gas sensing properties of the films were then comprehensively studied with respect to reducing gas resistance response at elevated temperatures, and also as a function of relative humidity changes when the films were maintained at room temperature.

Experimental

Nanopowder preparation and characterisation

Nanoscale powders of zirconia, alumina and tin dioxide were produced by focusing the pulsed output of a 1.2 kW Nd-YAG laser (Rofin Sinar RSY 1000P) onto the surface of a rotating ceramic rod of the relevant material held within an aggregation chamber followed by condensation of the induced vapour in a controlled atmosphere. This is shown schematically in Fig. 2. Ceramic rods of Al_2O_3 (Degussit, 99.7%) and ZrO_2 (Z-700, 3 mol% Y_2O_3 stabilised, >99%) were obtained from Friatec Ltd and BCE Special Ceramics Ltd respectively, while a SnO_2 ablation target was forged in-house from a powder supplied by Merck Ltd (extra purity grade 99.9%). The sample rod was fixed on a rotatable feedthrough driven by an electrical motor at 2 Hz. In addition, the aggregation chamber was mounted on a computer controlled linear manipulator, allowing the sample to be scanned by the laser beam along its rotating axis. In order to increase the powder production yield, the nanoparticles were generated in a sealed aggregation chamber and an aerosol was formed by introducing a clean air gas flow into the aggregation zone by means of a 1 mm diameter nozzle. The aerosol was then pumped through a filter system consisting of a glass fibre mesh in order to separate the airborne particles. The separation mechanism is largely governed by diffusion and attraction of the particles onto the surface of the glass fibres. By installing two filters in series, it could be demonstrated that more than 99% of the powder is collected at the first filter.

X-Ray powder diffraction analysis of the ablated powders showed that the Al_2O_3 is crystallised in the gamma form, while the ZrO_2 particles are formed in the tetragonal form. The tin oxide powder is a mixture of SnO_2 (cassiterite) and SnO (romarchite), although after heat treatment in air at temperatures up to 400 °C, all of the monoxide is transformed to the dioxide. The characteristics of Al_2O_3 and ZrO_2 powders after moderate heat treatment were not studied, although in the case of the latter it is possible that a phase transition of the tetragonal form to the more favoured monoclinic structure may occur. Transmission electron micrographs of the powders show that the nanoparticles are generally spherical in shape. Further analysis revealed that the particle size distributions of each of the three powders are logarithmic normal in nature with a standard geometric deviation of typically 1.8. For both Al_2O_3 and ZrO_2 powders, the median particle size is 13 nm, while the tin dioxide particles are larger at approximately 20 nm.

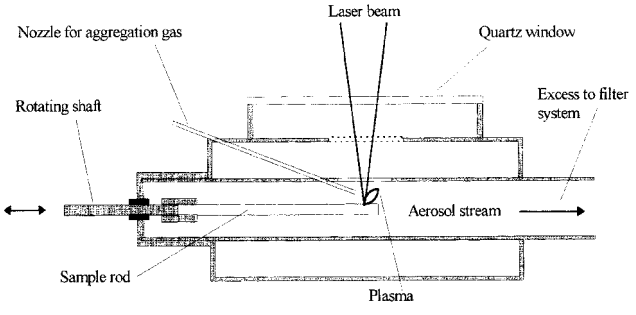

Fig. 2 Schematic representation of the laser evaporation chamber

Gas sensor preparation

Different methods of depositing nanopowders on to conventional 5 × 5 mm planar alumina substrates were investigated in order to produce consistent thick films, which could then be sintered resulting in the necessary mechanical stability. The usual method involves mixing the material with α-terpineol containing an ethyl cellulose viscosity regulator, to give an ink which can be either screen printed or wire dropped over the electrode array of a substrate. Slow drying of the ink below 100 °C leaves a continuous thick powder film ready for sintering. Experiments carried out on 0.1 g quantities of both ZrO_2 and Al_2O_3 nanopowders showed that this method was not suitable for producing satisfactory films. A minimum 0.2 cm^3 volume of organic medium was required to form a gelatinous ink of the material which, upon drying, underwent significant shrinkage and subsequent severe film cracking. More satisfactory results were obtained by dispersing the powders in distilled water to give suspensions of approximately 200 mg cm^{-3}. Thick films were prepared by repeatedly dropping 10 μl aliquots of the suspension on to the surface of planar alumina substrates heated to 80 °C. After drying, the sensors were sintered at 600 °C for 5 h in air prior to testing. Sensing elements were also prepared from pressed pellets of both nanoscaled oxide powders, which were subjected to sintering at different temperatures in the range 850–1500 °C. Subsequent wire attachments were made by means of a conductive Pt adhesive which was cured at 800 °C for 1 h.

Thick films of nanocrystalline tin dioxide were less prone to cracking and therefore easier to prepare. Gas sensitive films were formed by ultrasonically dispersing the powder in an aqueous medium and applying a single 10 μl drop of the dispersion over the electrode array of an alumina substrate. By this method a range of films of different thicknesses, calculated to be in the region 12 μm down to less than 1 μm could be formed by using dispersion concentrations in the range 200 to 12 mg cm^{-3}. It was noted that the use of dispersions of >200 mg cm^{-3} concentration caused cracks to form within the films upon drying. A similar result was observed when attempts were made to prepare thick films by repeated deposition and drying of 10 μl aliquots of the dispersions. After drying, the films were heat treated in air for a 2 h period at temperatures ranging from 400–1000 °C, prior to testing.

Results and Discussion

Alumina thick film and pressed pellet sensors

The resistance response of thick film sensors prepared from both nanosized and commercially available microcrystalline powders (B.D.H. 99.99%, 0.3 μm particle size) to reducing gases such as hydrogen, carbon monoxide and methane at elevated temperatures were studied. As expected in the case of the commercially available powder, no resistance changes could be detected upon exposure to the test gases. Sensors prepared from nanopowder were also unresponsive to both CO and methane, though a reversible 40% drop in resistance could be observed upon introducing a 1% v/v hydrogen con-

centration into the test chamber at operating temperatures in the range 400–600 °C.

In separate experiments the room temperature resistance and capacitance response of both types of sensor as a function of relative humidity (R.H.) (0–98%) were studied. This was achieved by introducing the sensors into the headspace above a range of saturated salt solutions maintained at 20 °C. Porous metal oxide ceramics are well known as sensor materials which display a conductivity change when the relative humidity of the ambient changes.[10] This is caused by capillary condensation of water vapour within the micropores of the material. Proton transfer between neighbouring water molecules accounts for the conductivity increase as the relative humidity is raised. Experiments showed that both thick film alumina sensor types responded markedly to changes in R.H. Fig. 3 shows that capacitance/resistance changes of up to five orders of magnitude were observed over the 0–98% R.H. range. In general the nanosized material exhibited the greatest response to low humidities while the commercial powder responded more markedly at higher humidities. The results of experiments on the dynanic response of the alumina thick films to step-like increases and decreases in humidity are given in Fig. 4. The response and recovery times for the nanocrystalline sample appear to be markedly longer than for the commercial alumina, probably reflecting the added restriction on the diffusion of water vapour to the film bulk, as a consequence of decreasing pore size. These observations appear to be consistent with predicted sensor behaviour based on a pore size distribution influenced model proposed by Seiyama *et al.*[10] Here the porous ceramic thick film is considered as a network of capillaries arranged perpendicularly to the measuring electrodes. The model predicts that resistance–humidity characteristics of small

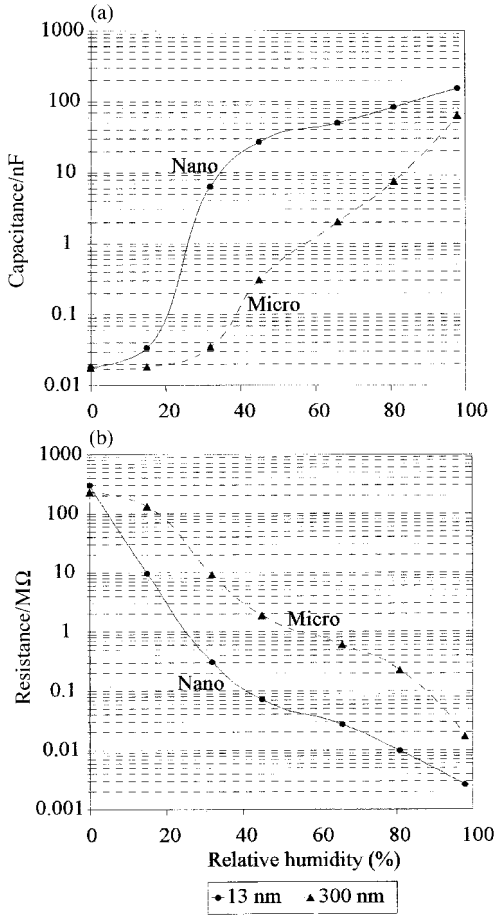

Fig. 3 A comparison of the observed changes in (a) capacitance and (b) resistance as a function of relative humidity at 20 °C for both types of alumina based sensor

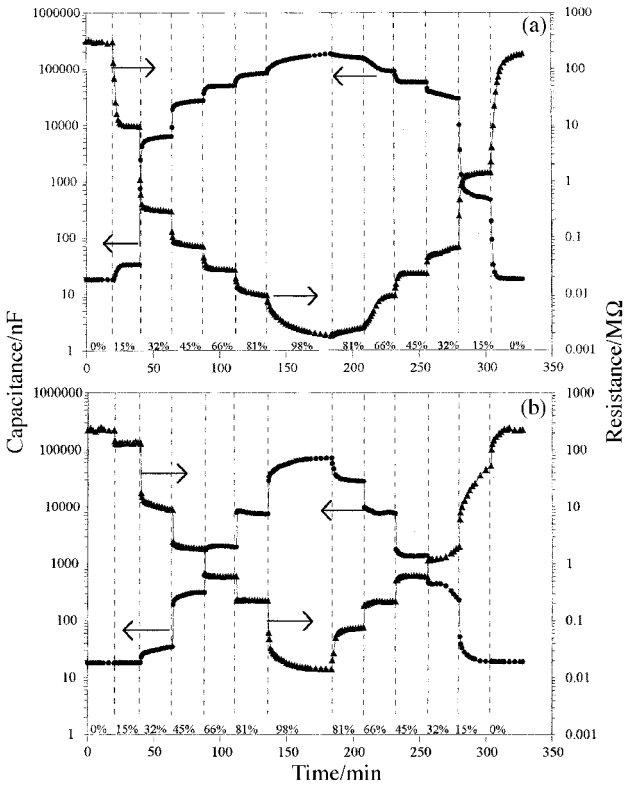

Fig. 4 Dynamic response of thick sintered films of (a) nanosized and (b) commercially available alumina powder to changes in relative humidity at 20 °C

pore size materials, such as nanocrystalline oxides, are only affected by changes in the low humidity range. Conversely, larger pore sizes give rise to a sensor which is unresponsive until a certain high humidity threshold is reached.

Humidity response characteristics were also determined for sensor elements formed from sections of a pressed pellet of nanoalumina, sintered at different temperatures in the range 850–1500 °C, and typical results are illustrated in Fig. 5. Tests showed that the dc resistance and capacitance of the n-Al_2O_3 ceramics also changed markedly over the 0–98% R.H. range. Again a total change of approximately five orders of magnitude was observed for the resistance of the sample, while the capacitance varied by approximately three orders of magnitude. The response characteristics for the n-Al_2O_3 pellets differ from those observed for thick powder based films, in that little change occurs upon increasing humidity from 0–20% RH, with the majority of response occurring in the 20–60% RH range. It was also noted that the response time of the pellet based sensors was significantly shorter than corresponding thick film devices. Increasing the sintering temperature of the pellet did not lead to any decrease in the overall resistance change but caused a more pronounced step-like change in the response curve in the 20–40% RH range.

The dependence of humidity response on sintering temperature was even more marked for n-Al_2O_3 pellets which were impregnated with LiCl prior to testing and these results are shown in Fig. 5(b). This was achieved by immersing the pellets in a 5% w/v aqueous LiCl solution for 1 h prior to drying at 100 °C and subsequent high temperature sintering. The addition of alkali metals to ceramic thick films is a common method of improving humidity sensing characteristics and is thought to increase the number of water adsorption sites available as well as acting as a sintering agent.[11] SEM photographs of the alumina pellets reveal that increasing the heat treatment temperature above 1100 °C leads to neck formation between the grains of the material. As sintering proceeds,

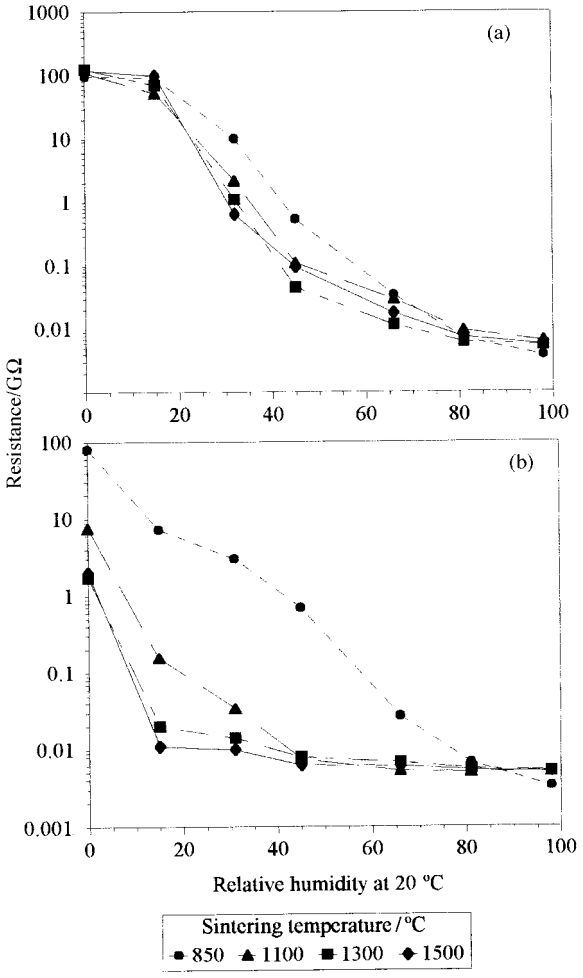

Fig. 5 Changes in dc resistance as a function of relative humidity at 20 °C for a series of (a) undoped and (b) LiCl doped nanoalumina pressed pellets sintered at different temperatures in air for 5 h

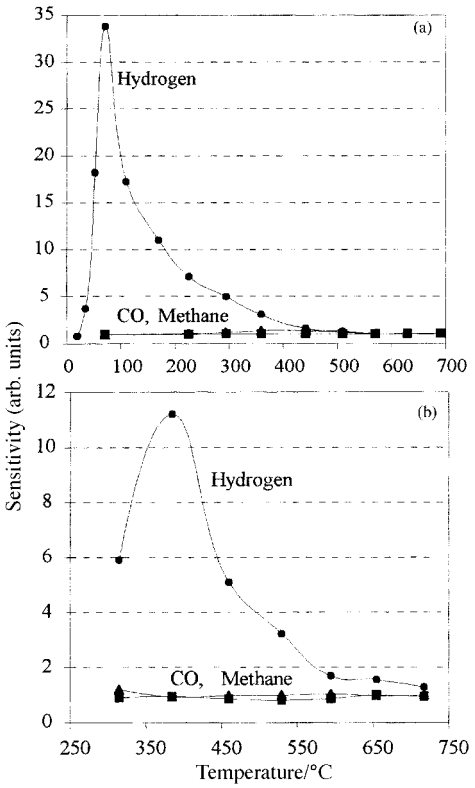

Fig. 6 Plots of sensitivity *versus* operating temperature for sintered thick films of (a) nanosized and (b) commercially available zirconia powder. A fixed reducing gas concentration of 1% v/v in dry air was used throughout and the sensors heat treated at 600 °C for 5 h prior to testing. It should be noted that sensitivity is defined as the ratio R_{air}/R_{gas}, where R_{air} is the sensor resistance in clean air and R_{gas} is the resistance in the test gas.

although the porosity of the material decreases, the sizes of the remaining pores also decrease significantly. The observed changes in resistance–humidity characteristics of the sintered Li-doped alumina ceramics, especially samples heat treated at 1300 °C or higher, are again consistent with a progressive decrease in pore size where 90% of the observed resistance change occurs in the 0–20% R.H. range.

Zirconia thick film and pressed pellet sensors

The reducing gas sensitivity of thick film sensors prepared from both nanosized and commercial ZrO_2 powders were studied as a function of operating temperature. A comparison of the sensing characteristics of both sensors is shown in Fig. 6, where sensitivity is represented as the ratio of sensor resistance in clean air to that observed in test gas. Both devices remain unresponsive to 1% v/v concentrations of either CO or methane over the whole operating temperature test range. However, a marked response to hydrogen is displayed by both sensors, though at markedly different operating temperatures. The nanopowder responds over the range 50–350 °C with optimum sensitivity occurring at 80 °C where a 30-fold change in resistance is observed. A maximum 10-fold resistance change is displayed by the commercial powder at a temperature of 400 °C. As in the case of alumina, the resistivity of the nanopowder is over three orders of magnitude lower than the commercially available material. However, despite this, the resistances of the sensors at their respective optimum operating temperatures exceed $10^9\Omega$, thus making accurate gas sensitivity measurements difficult. For effective use of polycrystalline nano-ZrO_2 in a chemoresistive thick film, the electrical conductivity must be increased. Commonly used sensor materials such as tin dioxide, which exploit bulk resistance modulations brought about by surface phenomena, can be modified by the incorporation of an electron donating additive such as Sb^{III} to produce a decrease in sensor resistivity to a more manageable level.[12,13] Hence, there is a requirement for an additive which can perform a similar function for zirconium oxide. However, given that its use as a solid state electrolyte in high temperature oxygen detection is the main sensing application of ZrO_2, most research output in this area has been directed towards improving its oxygen ion conductivity.[14] Consequently, since researchers have striven to minimise the electronic conductivity of ZrO_2, there is no mention in the literature of methods for increasing this property. In addition, given the highly ionic nature of ZrO_2, it is unlikely that its electronic properties would be influenced by electron donating additives in the same manner as a semiconducting oxide such as SnO_2. Therefore, in the absence of an established method of reducing its resistivity, a hydrogen sensitive varistor based on nanocrystalline ZrO_2 has little commercial value.

Humidity tests on sensor elements composed of n-ZrO_2 pellets, sintered at different temperatures in the range 850–1500 °C, produced similar characteristics to those described previously for n-alumina. The greatest resistance changes occur in the 30–80% RH range, while an increase in sintering temperature produces a shift in the region where the most marked change takes place. For example, a pre-treatment temperature of 850 °C causes a marked resistance fall between 30 and 40% RH, while sintering at 1500 °C leads to a step-like resistance change between 65 and 80% RH.

All sensors prepared were initially tested with respect to their resistance response to 1% v/v mixtures of CO, methane and hydrogen in air over a wide range of operating temperatures up to a maximum of 600 °C. Optimum detection temperatures were determined and sensors maintained at this fixed temperature were exposed to varying concentrations of test gases.

Preliminary experiments were carried out on thick sensing films prepared from powder samples of laser ablated, commercially available (Keeling and Walker Ltd., 99.999%), and conventionally prepared tin dioxide, using a pre-treatment temperature of 700 °C. The latter was produced *via* the controlled hydrolysis of an aqueous $SnCl_4$ solution followed by calcination at 700 °C and milling of the α-stannic acid gel obtained. A similar method is used to produce tin dioxide powders which form the basis of most commercial semiconductor gas sensors, and has previously been comprehensively characterised by the authors.[15] Both nano-SnO_2 and conventionally prepared samples were considerably more sensitive than the commercially available sample by up to a factor of five. Fig. 7 shows that although the nanopowder is generally more sensitive than conventionally prepared samples to all three test gases, the difference is not significant. Optimum detection temperatures for each of the individual gases occur at the same point within the test range. The fact that both nanocrystalline and conventionally prepared powders behave in a similar manner is not unexpected. Although SEM analysis of the latter shows micron-sized grains, these are in fact aggregates composed of smaller crystallites in the 20–100 nm diameter range.[1,2] Although the particle sizes of the primary grains of the two SnO_2 powders are similar, there are other significant differences which may account for the superiority of the nanocrystalline material. Films prepared from conventional SnO_2 powders are liable to be influenced by two types of intergrain contact. First, a larger number of contacts between neighbouring crystallites which comprise each aggregate, and secondly a smaller number of boundaries between each aggregate which exercise the main control over film conductance. In contrast, aggregate formation in the case of nanocrystalline SnO_2 thick films is restricted to soft agglomerates which may form in aqueous dispersion precursors, but can be broken up by a combination of ultrasound and stirring. Therefore, only one type of intergrain contact is likely to be present, and assuming reacting gases can diffuse without restriction throughout the bulk, each of the SnO_2 particles present can exert an influence on the final film resistance.

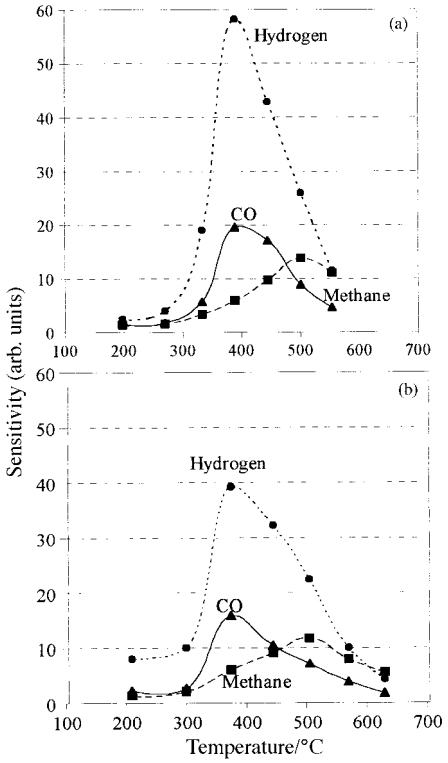

Fig. 7 A comparison of the performance of (a) nanocrystalline and (b) conventionally prepared SnO_2 samples deposited on gas sensor substrates. A test gas concentration of 1% v/v in dry air was used.

Two types of experiment were carried out to optimise factors which are likely to have the greatest influence on the performance of nanocrystalline SnO_2 thick films. In the first experiment, a series of sensors having a constant n-SnO_2 film thickness of 12 μm were heat treated in air for 2 h at different temperatures within the range 400–1000 °C. Maximum sensitivity to the three test gases was then determined as a function of the initial heat treatment temperature and the results are shown in Fig. 8. It appears that CO sensitivity is most markedly influenced by changing the sintering temperature. The use of a firing temperature of 700 °C gives rise to a sensing film which is twice as sensitive as the same n-SnO_2 material heat treated using temperatures at the extremes of the test range. In contrast, both CH_4 and H_2 response was not unduly influenced by sintering temperature, although for all gases, the use of the highest temperature of 1000 °C caused a significant decrease in sensitivity. SEM analysis of the sintered films showed that the SnO_2 films deposited from an aqueous medium consist of clusters of nanoparticles which are *ca.* 20–50 nm in diameter for heat treatment temperatures of 700 °C or less. As the firing temperature is raised, sintering is initiated where the average grain size increases, until at the maximum temperature of 1000 °C, many of the grains have a diameter of 100 nm or greater. SEM photographs of these observations are presented in Fig. 9. The extent of grain growth observed here appears to be significantly less pronounced than reported by others[3,9] over a comparable temperature range. The difference in behaviour in one of these cases is probably due to a size effect, where sintering of a SnO_2 powder of 8 nm particle size[9] is more likely to occur at a lower temperature than a 20 nm median grain size sample. In the second instance,[3] given that the reported particle size of 17 nm is similar to the laser ablated SnO_2 powder studied here, the discrepancy probably arises because of the difference in powder preparation. It is highly likely that the properties of materials prepared by calcining α-stannic acid gel,[3] such as the degree of surface hydroxylation, will differ considerably from the anhydrous nanosized SnO_2 sample employed in this study.

Pre-treatment temperature also has a profound effect on the resistance–operating temperature characteristics of the n-SnO_2 films in clean dry air, as illustrated in Fig. 10(a). Each of the

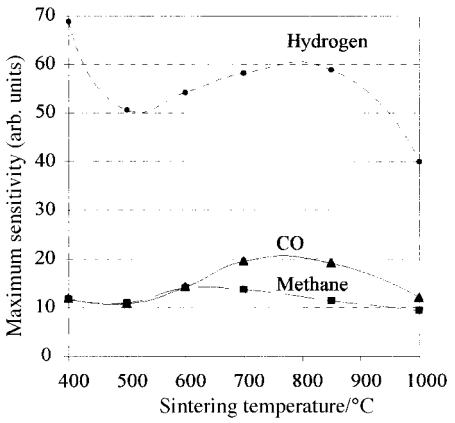

Fig. 8 Optimisation of sensitivity to a 1% v/v test gas concentration with respect to sintering temperature for a series of nano-SnO_2 sensors employing a film thickness of 12 μm

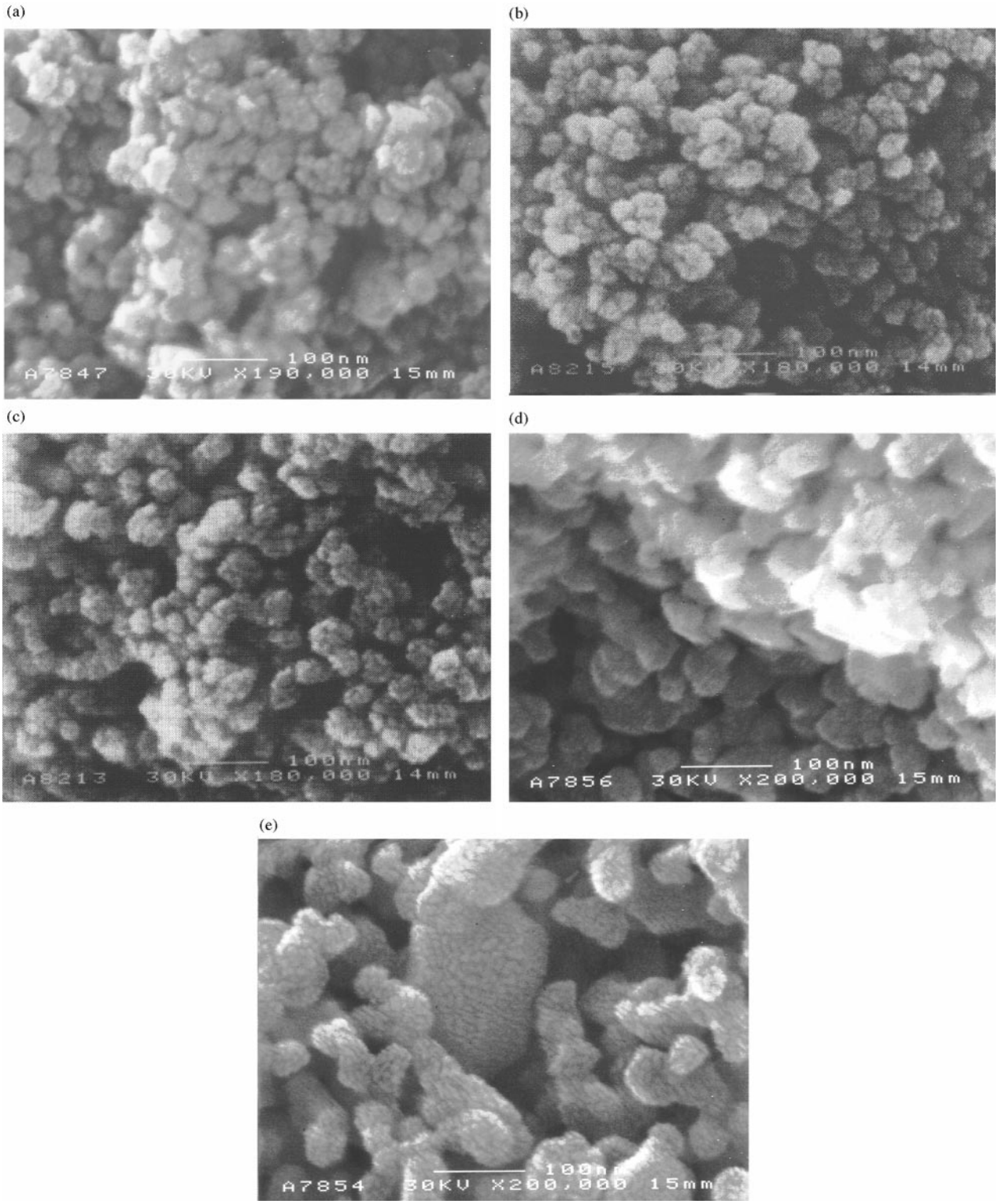

Fig. 9 SEM photos of nanocrystalline SnO_2 thick films heat treated at temperatures of (a) 500, (b) 600, (c) 700, (d) 850 and (e) 1000 °C for 2 h in air

films studied displays a negative temperature coefficient of resistance in the range 400–600 °C. However, for samples fired at 700 °C or lower, decreasing the operating temperature below 400 °C causes film resistance to reach a maximum at *ca.* 350 °C. This then falls as the temperature is decreased further. The use of higher pre-treatment temperatures leads to a gradual disappearance of this behaviour, where the drop in clean air resistance below 350 °C is eventually replaced by a slight inflection in the resistance–temperature plot. Similar observations have been previously reported for porous SnO_2 pressed pellets and tentatively ascribed to a possible $O^- \leftrightarrow O^{2-}$ transformation which involves a doubling of the surface charge.[16] However, given that the starting material in the present study is a mixture of SnO_2 and SnO, as revealed by XRD analysis, an alternative explanation for this behaviour may lie with the extent of film non-stoichiometry. The region of positive temperature coefficient behaviour observed for films fired at 700 °C or less occurs when shallow donor levels are completely ionised, and subsequent temperature increases serve only to impart existing conduction band electrons with extra thermal energy, leading to increased resistivity. This continues until a threshold temperature is attained, sufficient to allow promotion of electrons from deeper lying oxygen surface states, thus causing a decrease in resistivity with increasing temperature.

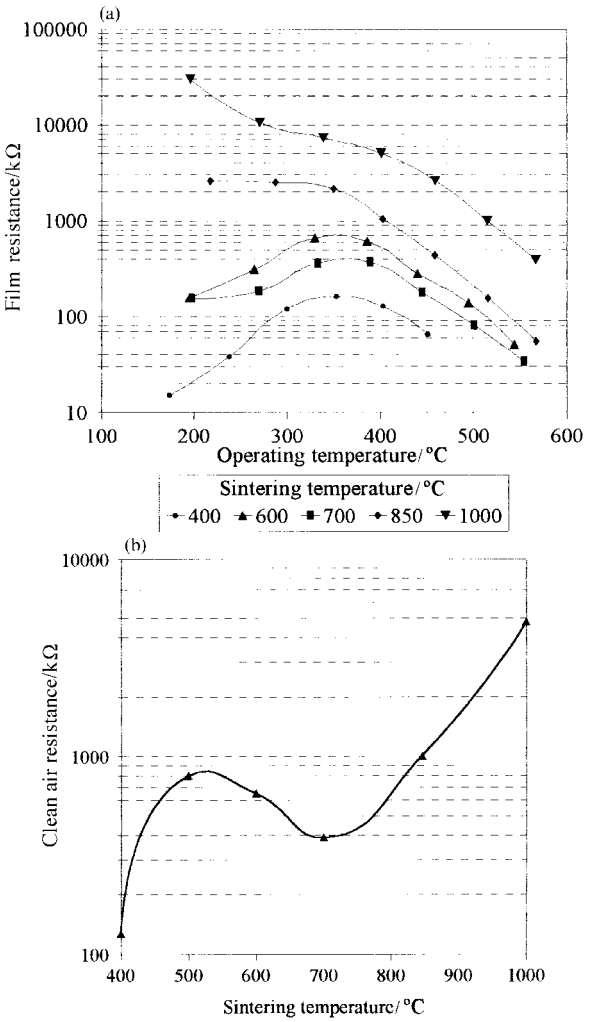

Fig. 10 The effect of firing temperature on the clean air resistance characteristics of nanocrystalline SnO_2 thick films illustrated by plots of (a) resistance *versus* operating temperature and (b) clean air resistance at fixed operating temperature of 400 °C as a function of firing temperature

In general a rise in the resistivity of the n-SnO_2 films accompanies an increase in firing temperature, signifying that the shallow lying donor levels caused by lattice oxygen vacancies are being eliminated. High temperature firing therefore produces irreversible changes in the stoichiometry of the SnO_2, whereby atmospheric oxygen fills lattice vacancies initially present in the laser ablated material. However, a plot of clean air resistance as a function of pre-treatment temperature [Fig. 10(b)], at the normal operating condition of 400 °C, shows anomalous behaviour in the region 500–700 °C. Here, resistance drops as the sintering temperature is increased. A possible explanation may be that this region represents the onset of sintering, though not detected by SEM analysis, which improves the intergranular contact, thus reducing the barrier to electron transport. Therefore the plot illustrated in Fig. 10(b) is probably the result of two competing processes. At firing temperatures of greater than 700 °C, the effects of irreversible stoichiometry changes dominate the improvement of electron transport due to sintering, while the converse is true at pre-treatment temperatures of less than 700 °C. Activation energies can be calculated from Arrhenius type plots of clean air resistance–operating temperature data in the range 400–600 °C, for films sintered at >700 °C. Linear ln R *vs.* $1/T$ relationships produce slopes which correspond to the ionisation energy of surface states produced by adsorbed oxygen, positioned approximately 1 eV below the conduction band. Values of

Table 1 The effect of firing temperature on various n-SnO_2 thick film parameters calculated from resistance *versus* operating temperature and resistance *versus* gas concentration data

pre-treatment temperature/°C	Arrhenius slope/eV	β (CO)	β (H_2)	β (CH_4)
400	—	0.42	0.65	0.39
600	—	0.46	0.64	0.43
700	0.91	0.47	0.63	0.40
850	1.04	0.48	0.67	0.40
1000	1.0	0.41	0.60	0.35

between 0.9 and 1.05 eV are observed for nanocrystalline SnO_2 films and are presented in Table 1. These correspond well with previous findings for conventionally prepared tin dioxide samples.[15,16] Sensor films which were sintered at temperatures of 600 °C or less did not display linear Arrhenius plots in the same region. Further experiments on the film response to varying concentrations of CO, H_2 and CH_4 at their predetermined optimum operating temperatures, revealed that firing temperature had little effect on sensing characteristics. Each of the films tested obeys a power law relationship of the type $R \propto [\text{gas}]^{-\beta}$, where β is the power law coefficient, for all three test gases. Values of β calculated in the 10–1000 ppm concentration range for each of the test gases are also listed in Table 1. It is evident that although sintering temperature has a profound effect on sensor resistivity, the power law coefficient remains unaffected, with the exception of a slight decrease at the highest pre-treatment temperature used. Exposure to gas concentrations in excess of 1000 ppm causes deviations in the power law relationship, and this concurs with the findings of others.[17] Actual β values observed in CO and CH_4 correspond well with values obtained previously for sintered thick films prepared from conventional SnO_2 powder samples,[15] although a typical power law coefficient of 0.9 reported for hydrogen is markedly higher than for the nanocrystalline material.

A second optimisation experiment involved the preparation of a series of sensing films of varying thickness, ranging from a minimum of 0.5 μm to a maximum of 12 μm on fixed 5 × 5 mm substrates. All sensors were heat treated at a temperature of 700 °C for 2 h, corresponding to the optimum determined by the previous study. Gas sensitivity tests, involving 1% v/v test gas mixtures in dry air, showed that decreasing the mass of active material by over an order of magnitude has little effect on both CO and H_2 sensitivity. However, the results

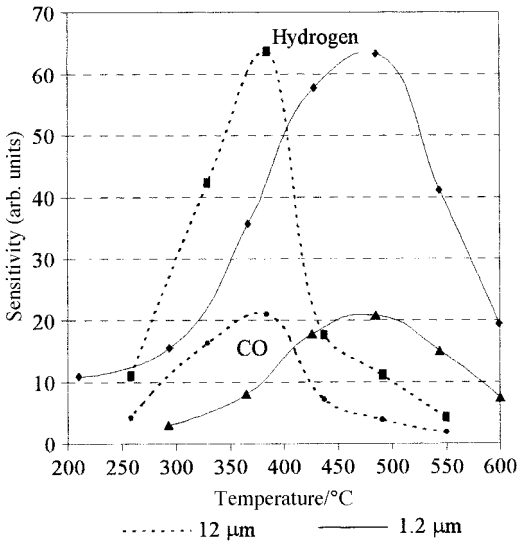

Fig. 11 Operating temperature optimisation plots obtained for n-SnO_2 films of two different thicknesses upon exposure to 1% v/v concentrations of CO and H_2 in dry air

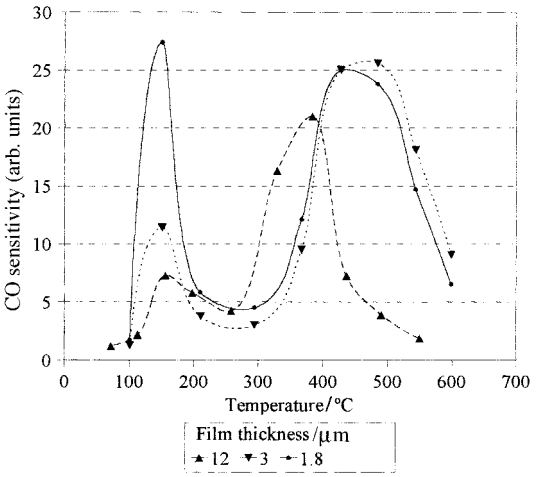

Fig. 12 Plots showing the onset of a dual CO response of n-SnO_2 films as film thickness is decreased. A test gas concentration of 1% v/v in dry air was used in each case.

show that a marked increase in CH_4 response can be obtained by employing an SnO_2 film of *ca.* 1.5–2.5 μm. Other notable effects are also observed upon decreasing the mass of the sensing film. Fig. 11 shows that as the sensing film thickness is decreased by a factor of 10, the optimum detection temperature increases significantly from 380 to 500 °C for both test gases. A second observation, revealed that sensitivity towards sub-1000 ppm levels of test gas increases noticeably as the sensing film thickness is decreased, even though the magnitude of sensor response to 1% v/v test gas mixtures remains relatively constant.

When the operating temperature range is extended below 250 °C, then the onset of an additional response to CO is observed which reaches a maximum at a temperature of 150 °C. Fig. 12 shows that as the film thickness is decreased, the magnitude of the CO sensitivity at this lower temperature increases markedly. Indeed, for a n-SnO_2 film thickness of 1.8 μm, the CO sensitivities observed at the two maxima of 150 and 500 °C are comparable. Exposure to CH_4 at 150 °C produces negligible resistance changes, whilst in the presence of H_2, the n-SnO_2 films display a remarkable p-type response, where resistance increases by factors of up to two orders of magnitude. The underlying reasons for his behaviour are unclear, though it is well known that a sensor temperature of 150 °C marks the point at which the nature of the ionosorbed surface oxygen species changes. EPR studies have shown that O_2^- surface species predominate at below 160 °C, while higher temperatures favour the adsorption of oxygen as O^-.[18] However, it is debatable whether or not this transformation has a direct influence on sensor behaviour, and most especially on the enhanced CO sensitivity observed in the 100–200 °C region, since it is widely considered that O_2^- surface species are markedly less reactive than O^-.[19]

Conclusions

A novel laser evaporation method for producing nanocrystalline gas sensing materials has been developed. Although sensors prepared from thick films of nanoscaled metal oxides such as SnO_2, ZrO_2 and Al_2O_3 behave in a similar manner to their micron sized counterparts, in general, gas sensing properties are improved. Thick film and pressed pellet alumina sensors display marked resistance and capacitance changes when exposed to varying relative humidity levels at room temperature. The morphology of the sensing material, which can be modified by the use of different firing temperatures, has a significant effect on the nature of the resistance *versus* humidity relationships. Similar behaviour was observed for ZrO_2 based sensors, although greater value has been placed on a hydrogen response at elevated temperatures, which in the case of the nanocrystalline sample occurs at a lower detection temperature and with a markedly higher sensitivity than commercially available material. Nanocrystalline SnO_2 sensors have been optimised with respect to both pre-treatment temperature and film thickness, and shown to respond to CO, H_2 and CH_4 in a similar manner to conventionally prepared samples, though with a moderate enhancement of sensitivity. However, although the improvement in performance is not significant at present, it is hoped that modification of the evaporation environment can lead to a further decrease in particle size of generated powders. For a sensing material such as SnO_2, should this be brought within a region where the depletion layer caused by chemisorption of gaseous species is equal to the radius of the particle, typically considered to be *ca.* 6 nm,[2] then a sizeable improvement in gas sensor response can be expected.

The authors would like to express their sincere thanks to Drs. Hans Ferkel and Werner Riehemann of the Technical University of Clausthal who provided the nanocrystalline samples and Dr. Patrick Keller of the Fraunhofer Institute, St. Ingbert, Germany who supplied the SEM data. This research is funded by the European Union as a part of its BRITE-EURAM programme, project number BE95-1989.

References

1 K. Ihokura and J. Watson, *The stannic oxide gas sensor–principles and applications*, CRC press, Boca Raton FL, 1994.
2 C. Xu, J. Tamaki, N. Miura and N. Yamazoe, *Sens. Actuators B*, 1991, **3**, 147.
3 A. Diéguez, A. Romano-Rodríguez, J. R. Morante, U. Weimar, M. Schweizer-Berberich and W. Göpel, *Sens. Actuators B*, 1996, **31**, 1.
4 M. Schweizer-Berberich, J. G. Zheng, U. Weimar, W. Göpel, N. Bârsan, E. Pentia and A Tomescu, *Sens. Actuators B, 1996,* **31**, 71.
5 G. Sberveglieri, *Sens. Actuators B*, 1995, **23**, 103.
6 P. Nelli, L. E. Depero, M. Ferroni, S. Gropelli, V. Guidi, F. Ronconi, L. Sangaletti and G. Sberveglieri, *Sens. Actuators B*, (1996), **31**, 89.
7 J. A. de Agapito and J. P Santos, *Sens. Actuators B*, 1996, **31**, 93.
8 D. G. Rickerby, M. C. Horillo, J. P. Santos and P. Serrini, *Nanostruct. Mater.*, 1997, **9**, 43.
9 V. M. Jiménez, A. R. González-Elipe, P. Espinós, A. Justo and A. Fernández, *Sens. Actuators B*, 1996, **31**, 29.
10 T. Seiyama, N. Yamazoe and H. Arai, *Sens. Actuators*, 1983, **4**, 85.
11 E. Traversa, *Sens. Actuators B*, 1995, **23**, 135.
12 G. S. V. Coles, G. Williams and B. Smith, *Sens. Actuators B*, 1991, **3**, 7.
13 L. N. Yannopoulos, *Sens. Actuators*, 1987, **12**, 77.
14 R. M. A. Kocache, in *Solid State Gas Sensors*, ed. P. T. Moseley and B. C. Tofield, IOP Publ. Ltd., Bristol, 1987, p. 1.
15 G. S. V. Coles and G. Williams, *J. Mater. Chem.*, 1992, **2**, 23.
16 J. F. McAleer, P. T. Moseley, J. O. W. Norris and D. E. Williams, *J. Chem. Soc., Faraday Trans. 1*, 1987, **83**, 1323.
17 P. K. Clifford and D. T. Tuma, *Sens. Actuators*, 1982/83, **3**, 233.
18 S. C. Chang, *J. Vac. Sci. Technol.*, 1980, **17**, 366.
19 V. Lantto and P. Romppainen, *Surf. Sci.*, 1987, **192**, 243.

Paper 8/02006J; *Received* 12*th March*, 1998